

## Population of excited He states ( $3 \leq n \leq 8$ ) by dielectronic He<sup>+</sup> recombination in dc hollow-cathode discharge

Ingrid Kuen, Franz Howorka, and Herbert Störi

*Institut für Experimentalphysik der Leopold-Franzens-Universität, A-6020 Innsbruck, Austria*

(Received 27 June 1980)

The contribution of dielectronic recombination to the population of radiative He I states ( $3 \leq n \leq 8$ ) in a He dc hollow-cathode discharge of 4-cm length and 2-cm diameter is determined in the discharge pressure range 0.6–4.0 Torr and at discharge current values of 10, 13, 16, 19, 22, and 25 mA by radial sampling of the emitted line radiation and the ion densities. In addition, the afterglow phase of the same discharge is explored as to the radial and time dependence of line radiation intensity and ion density. In the active phase at low density (2 Torr) and at higher pressure but at too low a discharge current (below 12 mA) all the radiation is due to electron impact excitation of the He states. Only at a pressure of about 4 Torr and a discharge current above 20 mA does recombination play a significant role in populating radiative He I states on the axis of the discharge. The radial dependence of the He II radiation shows the geometric density increase of the very fast unscattered electrons having the full sheath energy. Both results are relevant for hollow-cathode-laser development.

### I. INTRODUCTION

The recombination of helium ions in plasmas has been the topic of many investigations during the last decades. Most of these investigations were undertaken to measure the ion-electron recombination coefficients of the ion species present in the plasma. To exclude direct electron-impact excitation of the same states that are populated by recombination, all these investigations were undertaken in flowing or stationary afterglow plasmas. The experiments and their results are summarized in two review articles by H. J. Oskam<sup>1</sup> and by H. S. W. Massey and H. B. Gilbody.<sup>2</sup> A very extensive study of the processes in a helium afterglow has been described by R. Deloche *et al.*<sup>3</sup> The general opinion seems now to be adopted that dielectronic recombination of He<sup>+</sup> ions will populate the atomic He states that give rise to the observation of atomic lines whereas the recombination of He<sub>2</sub><sup>+</sup> yields mostly molecular bands. A dissociative recombination of He<sub>2</sub><sup>+</sup> to give excited He levels seems not to be effective.

In active dc plasmas, e. g., the negative glow of a cylindrical hollow cathode, all sorts of excitation mechanisms will occur at the same time and in the same volume. It is therefore not easy to distinguish between line radiation due to electron impact excitation of ground or excited states and the radiation coming from the same levels that have accidentally been populated by an electron-ion-recombination mechanism. That the recombination in the field-free region of the negative glow of a dc hollow cathode might be the reason for fine, narrow lines originating from high-lying states of different atoms has—according to oral tradition<sup>4</sup>—been suspected for a long time but it has never

been formulated or proved experimentally in the literature.

The experience our group has gained during the last few years concerning the ion balance in the negative glow of a hollow-cathode discharge in different gases and gas mixtures<sup>5–10</sup> has encouraged us to extend these investigations to the application of emission spectroscopy in addition to the mass spectrometric, space-resolved diagnostic method, using the same cylindrical hollow cathode. During the course of these investigations it proved necessary to include time-resolved measurements (stationary afterglow) as well. The result of all these investigations will be presented here and will show that we can indeed distinguish between the different processes that lead to the population of excited states, i. e., we can show when and where the population by recombination is dominant over that by electron impact or concurring processes. As a byproduct, the spectroscopic investigation of ionic He II lines gives some information on the spatial distribution of the fastest electrons in the discharge that traversed the cathode sheath and part of the negative glow without undergoing any collisions.

### II. EXPERIMENTAL

The ion-diagnostic apparatus has been described in detail<sup>11</sup> and therefore only a very brief summary will be given here. A cylindrical hollow cathode of 2-cm diameter and 4-cm length can be moved in radial direction with respect to a mass spectrometric sampling probe (diam 1 mm, diam of sampling orifice 50 μm). On the opposite end (through the hollow anode) a lens system (fused silica) images a small slab of the discharge (reso-

TABLE I. Wavelengths (in Å) of the lines observed in the hollow-cathode discharge.

a. Helium I					
$nd^3D-2p^3P$	$ns^3S-2p^3P$	$np^3P-2s^3S$	$nd^1D-2p^1P$	$ns^1S-2p^1P$	$np^1P-2s^1S$
3d 5876	3s 7065	3p 3888	3d 6678	3s 7281	3p 5015
4d 4471	4s 4713	4p 3187	4d 4921	4s 5047	4p 3968
5d 4026	5s 4120	5p 2945	5d 4387	5s 4437	5p 3613
6d 3819	6s 3867	6p 2829	6d 4143	6s 4168	6p 3447
			7d 4009		
			8d 3926		

b. Helium II	
$nf^2F^o-3d^2D$	
4f 4685	
5f 3203	
6f 2733	

lution 0.1 mm) to the entrance slit of a 0.5-m Ebert grating monochromator with Peltier cooled multiplier and subsequent single photon counting equipment.

A survey spectrum showed that the helium discharge emitted only atomic He I lines and atomic-ion He II lines at the pressures (0.6–4.0 Torr) and discharge currents (10–25 mA) used. There were no molecular bands observable under these conditions.

The radial distributions across the hollow cathode of the lines shown in Table I were recorded at pressures of 0.6–4 Torr and at discharge current values of 10, 13, 16, 19, 22, and 25 mA.

Mass spectrometric studies of the  $\text{He}^+$  and the  $\text{He}_2^+$  ion densities across the discharge were undertaken at the identical parameter settings simultaneously. In addition the time behavior of the line intensities and of the ion densities in the afterglow phase of the same discharge was studied, using a fast pulser which was developed earlier and is described elsewhere.<sup>12,13</sup>

### III. RESULTS

#### A. Intensities of He I lines

The line intensities along a radial coordinate through the cylindrical hollow-cathode discharge may be grouped following various principles. One obvious grouping is according to the discharge pressure and the discharge current. If we look for example for the intensity distribution of the  $np^3P-3s^3S$  series at 1.7 Torr and take 2 representative lines ( $3888 \text{ \AA}$ ,  $3p^3P-2s^3S$  and  $2829 \text{ \AA}$ ,  $6p^3P-2s^3S$ ), at the discharge current values indicated we obtain the distributions shown in Fig. 1. All the curves shown are similar. They have three maxima, two at the left-hand and the right-

hand glow edge, respectively, and one slight hump on the axis ( $r=0 \text{ mm}$ ). The maxima at the glow edges are clearly due to excitation by fast electrons streaming in from the cathode sheath (in this case the region from 6 to 10 mm), which traverse just the excitation maximum for the upper states of the lines at the curve maxima. Toward the interior of the negative glow which lies inside the glow-edge maxima the density and the energy of the fast electrons decreases, so a minimum is

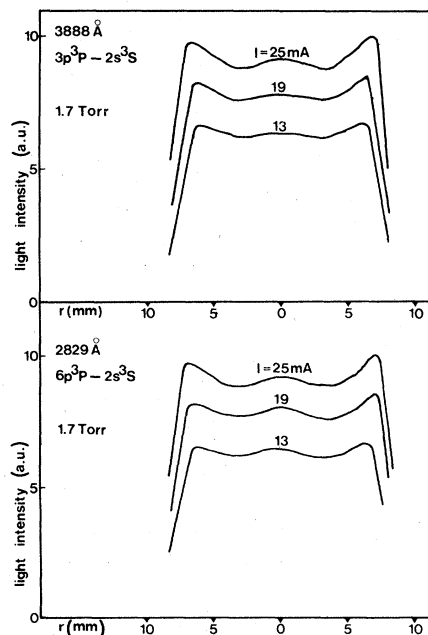


FIG. 1. Radial intensity distributions of two helium I lines in the active phase of the hollow-cathode discharge at a discharge pressure of 1.7 Torr and at discharge currents of 13, 19, and 25 mA.

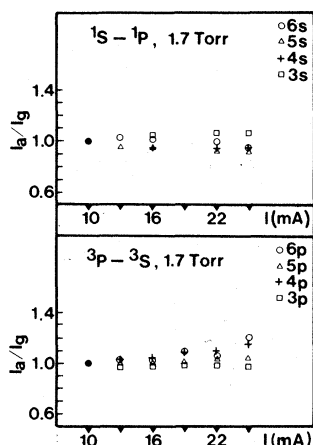


FIG. 2. Intensity ratios of  $I_a$ , the intensity on the axis, and  $I_g$ , the intensity at the sheath edge, for the  $ns^1S-1P$  and the  $np^3P-3S$  series of He I as dependent on the discharge current. The values are normalized at 10 mA.

formed in the interior of the negative glow. The small maximum on the axis may be due to a variety of processes (geometrical concentration of the fast electrons to form a "beam," see Sec. IIID; excitation from metastable states by plasma electrons, recombination, etc.), but this maximum is clearly due to similar processes as the glow-edge maxima. If we plot the intensity ratio  $I_a/I_g$  of the intensity on the axis,  $I_a$ , and that at the glow edges,  $I_g$ , normalized to the 10 mA value as a function of discharge current we obtain an approximately constant value for each line of each series (Fig. 2).

The appearance of the radial curves changes dramatically when the pressure is raised to 4 Torr. Figure 3 shows the respective curves for the triplet series (same representative lines as before) and for the  $ns^1S-2p^1P$  series (7281 Å,  $3s^1S-2p^1P$  and 4168 Å,  $6s^1S-2p^1P$ ).

At low discharge currents, the curves have only the maxima at the glow edge, which are—due to the higher pressure—shifted toward the cathode wall as compared to 1.7 Torr. No maximum of line intensity is observed on the axis. With increasing discharge current (or electron density in the interior of the negative glow), a strong maximum develops on the axis which is more pronounced for the higher states (6s and 6p) than for the lower ones (3s and 3p) and also for triplet lines as compared to singlet lines. Here definitely a different process sets in which favors the population of higher states on the axis as compared to the glow-edge values.

If we now plot the dependence of the intensity ratios  $I_a/I_g$  as functions of the discharge current and normalize these values to the values at 10-mA dis-

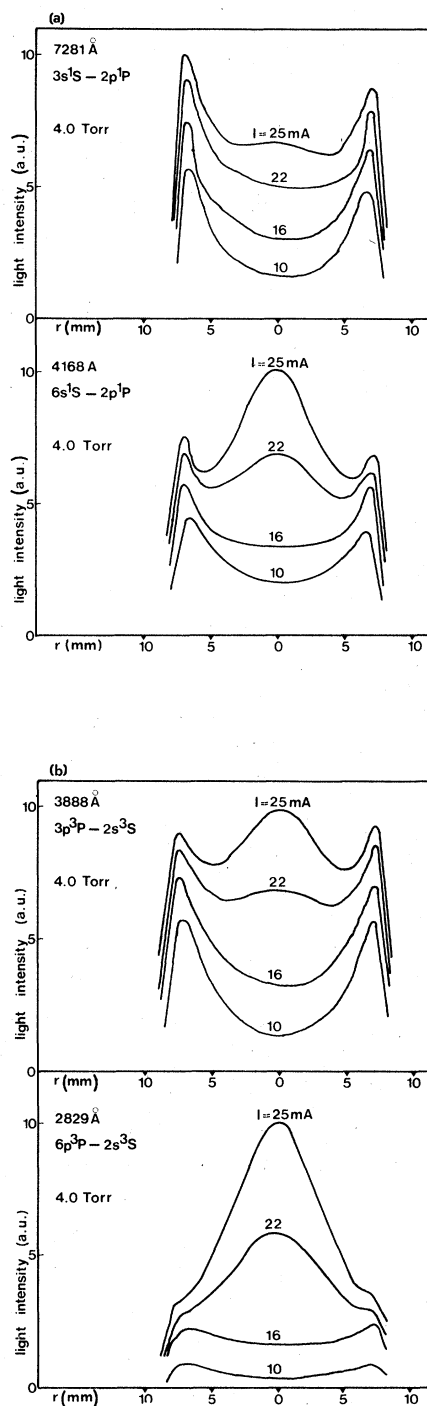


FIG. 3. (a) Radial intensity distributions of two helium I lines in the active phase of the hollow-cathode discharge at a discharge pressure of 4 Torr and at discharge currents of 10, 16, 22, and 25 mA, for the  $ns^1S-1P$  series. (b) Radial intensity distributions of two helium I lines in the active phase of the hollow-cathode discharge at a discharge pressure of 4 Torr and at discharge currents of 10, 16, 22, and 25 mA, for the  $np^3P-3S$  series.

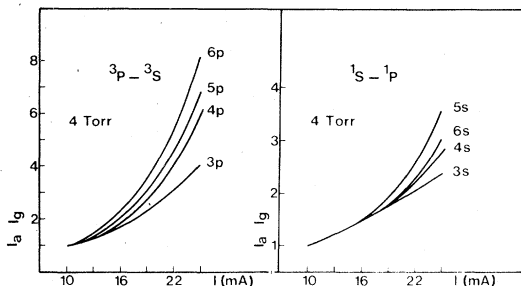


FIG. 4. Intensity ratios of  $I_a$ , the intensity on the axis, and  $I_g$ , the intensity at the glow edge, for the  $np^3P-3S$  and the  $ns^1S-1P$  series of He I as dependent on the discharge current. The values are normalized at 10 mA.

charge current as in Fig. 2, we obtain the curves shown in Fig. 4. The higher the principal quantum number  $n$ , the faster the maximum on the axis rises as compared to the one at the glow edge. The functional appearance is that of a parabola, i. e., the  $I_a/I_g$  ratio rises at least as the square of the electron density. A study of the intensity ratio  $I_a/I_g$  of the  $nd^1D-2p^1P$  lines as dependent on the discharge pressure (Fig. 5) shows that at low pressures the intensity on the axis as compared to that at the glow edge is lowest for the states with high principal quantum number  $n$  and high for the lower states, consistent with the population mechanism by electron impact excitation. With increasing pressure, however, the decrease of the  $I_a/I_g$  values is not uniform: Whereas the 3, 4 and 5d line intensities decrease about linearly, the state with higher  $n$  values lines decrease faster first, but then level off. At 4 Torr, the order of the intensity ratio values is reversed as compared to the values at 1 Torr. Now the states 6d-8d are favored against the states 3d-5d. Again this shows the influence of a process that is completely different from the electron impact excitation.

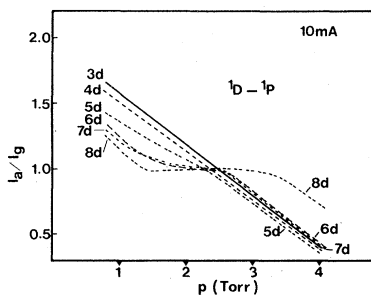


FIG. 5. Pressure dependence of the ratio of  $I_a$ , the intensity on the axis, and  $I_g$ , the intensity at the glow edge, for the  $nd^1D-1P$  series of He I at a discharge current of 10 mA.

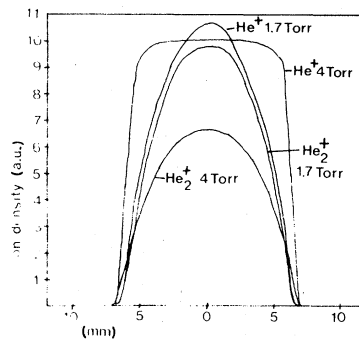


FIG. 6. Radial ion density distributions of the ions  $\text{He}^+$  and  $\text{He}_2^+$  at discharge pressures of 1.7 and 4 Torr.

### B. Ion density studies

The radial density distribution of  $\text{He}^+$  and  $\text{He}_2^+$  ions in the hollow-cathode discharge is shown for the pressure 1.7 and 4 Torr at a discharge of 25 mA in Fig. 6. The bell-shaped density distributions at the pressure of 1.7 Torr show that both ions suffer mainly diffusion losses. At 4 Torr the main loss for  $\text{He}^+$  besides diffusion is the termolecular reaction to form  $\text{He}_2^+$  and recombination with electrons; the main loss for  $\text{He}_2^+$  is still diffusion. Recombination of  $\text{He}_2^+$  is still weak at 4 Torr. The absolute  $\text{He}_2^+$  density as compared to the  $\text{He}^+$  density is about 10%. The steady-state conditions for the ions  $\text{He}^+$  and  $\text{He}_2^+$  read as follows:

$$\begin{aligned} d[\text{He}^+]/dt = 0 &= k_f[e_f][\text{He}] + D_{a,1}\nabla^2[\text{He}^+] \\ &\quad - k_3[\text{He}^+][\text{He}]^2 - \alpha[\text{He}^+][e_s]^2, \\ d[\text{He}_2^+]/dt = 0 &= k_3[\text{He}^+][\text{He}]^2 + D_{a,2}\nabla^2[\text{He}_2^+] \\ &\quad - \alpha_1[\text{He}_2^+][e_s]^2 - \alpha_2[\text{He}_2^+][\text{He}][e_s]. \end{aligned}$$

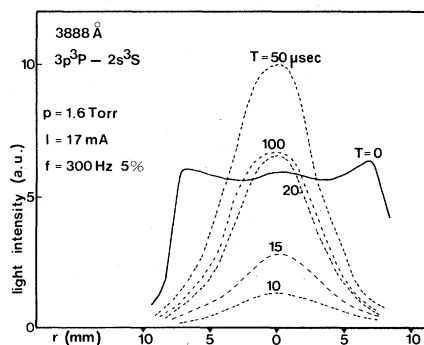


FIG. 7. Light intensity distribution across the negative glow of the hollow-cathode discharge at a pressure of 1.6 Torr and a discharge current of 17 mA for the He I 3888-Å line in the active phase ( $T=0$ ) and at after-glow times of 10, 15, 20, 50, and 100  $\mu\text{sec}$ . The discharge was pulsed with a frequency  $f$  of 300 Hz at a duty cycle of 5%.

Here, brackets denote number densities;  $D_{a,1}, D_{a,2}$  = ambipolar diffusion coefficients of  $\text{He}^+$  and  $\text{He}_2^+$ , respectively;  $k_f$  = rate constant for electron-impact ionization of He by fast electrons  $e_f$ ;  $k_3$  = termolecular conversion rate constant of  $\text{He}^+$  into  $\text{He}_2^+$ ;  $\alpha$  = dielectronic recombination coefficient of  $\text{He}^+$ ;  $\alpha_1, \alpha_2$  = electron and neutral stabilized recombination coefficients of  $\text{He}_2^+$ . The evaluation follows a scheme used in earlier cases and described in Refs. 5-7, 9, and 11.

Inserting the respective value for a pressure of 4 Torr, a discharge current of 25 mA, gas temperature  $T_g = 300$  K, and electron temperature  $T_e \approx T_g$ , and taking the values for the rate constants and recombination coefficients from the Deloche *et al.* paper,<sup>3</sup> i. e.,

$$\begin{aligned} k_3 &= 5.36 \times 10^{-32} \text{ cm}^6 \text{ s}^{-1}, \\ \alpha &= (6 \pm 2) \times 10^{-20} \text{ cm}^6 \text{ s}^{-1}, \\ \alpha_2 &= (5 \pm 1) \times 10^{-27} \text{ cm}^6 \text{ s}^{-1}, \\ \alpha_1 &= (4.0 \pm 0.5) \times 10^{-20} \text{ cm}^6 \text{ s}^{-1}, \\ k_f &= 2 \times 10^{-8} \text{ cm}^3 \text{ s}^{-1}, \\ D_{a,1} &= 112 \text{ cm}^2 \text{ s}^{-1}, \\ D_{a,2} &= 180 \text{ cm}^2 \text{ s}^{-1}, \end{aligned}$$

we obtain the important conversion rates in  $\text{cm}^{-3} \text{ s}^{-1}$ :

$$\begin{aligned} \text{diffusion loss of } \text{He}^+ &- 4.5 \times 10^{11}, \\ \text{diffusion loss of } \text{He}_2^+ &- 8.5 \times 10^{12}, \\ \text{ionization rate of He} &- 1.3 \times 10^{13}, \\ \text{three-body conversion of } \text{He}^+, \text{ into } \text{He}_2^+ &- 1.1 \times 10^{13}, \\ \text{recombination of } \text{He}^+ &- 3.1 \times 10^{11}, \\ \text{recombination of } \text{He}_2^+ &- 2.1 \times 10^{11}. \end{aligned}$$

The recombination of  $\text{He}_2^+$  is comparable to that of  $\text{He}^+$  but does not appear in the line radiation. Assuming now that the dielectronic recombination of  $\text{He}^+$  ions is an effective means to populate the upper levels of the transitions observed in Sec. II allows us to establish the steady-state equation of excited He atoms:

$$\begin{aligned} d[\text{He}^*]/dt = 0 &= k_f'[\text{He}][e_f] \\ &+ \alpha[\text{He}^+][e_s]^2 - [\text{He}^*]/\tau. \end{aligned}$$

Here,  $\tau$  is the lifetime of the excited  $\text{He}^*$  states ( $10^{-8}$  s). The  $k_f'$  values for electronic excitation by fast electrons were taken from St. John *et al.*<sup>14</sup> These values and the recombination rates from above give an estimate of the relative importance of population by  $\text{He}^+$  recombination and electron impact excitation:

$$\begin{aligned} \text{electron impact excitation} &- 5.8 \times 10^{11} \text{ cm}^{-3} \text{ s}^{-1}, \\ \text{dielectronic recombination} &- 3.1 \times 10^{11} \text{ cm}^{-3} \text{ s}^{-1}. \end{aligned}$$

This estimate shows that the additional process

which populates the upper levels of the lines observed on the axis might well be the dielectronic recombination of  $\text{He}^+$ .

### C. Afterglow measurements

To get more insight into the contribution of recombination to the population of the upper states of the lines observed, the discharge was switched on and off repeatedly, using a fast pulser which has been developed earlier.<sup>12,13</sup> The discharge was pulsed at a repetition frequency of 300 Hz at a pressure of 1.6 Torr and an averaged discharge current of 17 mA (duty cycle 5%). The light intensity distribution was then recorded across the negative glow at times in the afterglow of 10, 15, 20, 50, and 100  $\mu\text{sec}$  after switchoff. Figure 7 shows the spatial intensity distributions of the  $\text{He I } 3888 \text{ \AA } 3p^3P-2s^3S$  line. At a time  $T=0$  (active dc discharge) the distribution has the three-humped appearance described in Sec. III A. Already 10  $\mu\text{sec}$  after switching off the discharge the humps at the glow edge have disappeared, indicating that they are due to electron impact excitation by fast electrons which have gone away immediately. The maximum of the light intensity on the axis, however, remains and grows in the time interval up to 50  $\mu\text{sec}$ , then the intensity drops again with a characteristic time constant. Figure 8 shows the time dependence of the intensity of some of these lines on the axis. Figure 9 compares the characteristic decay curves of the light intensity with the decay of the ion densities observed simultaneously by the mass-spectrometric probe. The time constant of the light intensity is about  $\frac{1}{3}$  that of the ion signal decay, consistent with Gerber *et al.*'s<sup>15</sup> observations in a helium afterglow. These authors explain the ratio of the decay constants by population of the upper states through dielectronic recombination of  $\text{He}^+$ ;  $\text{He}_2^+$  shows the

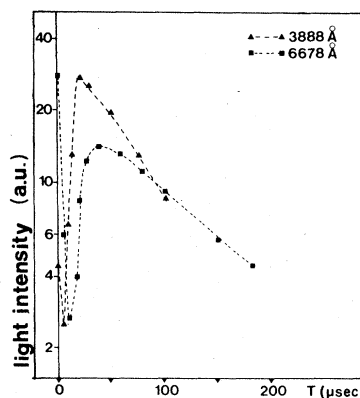


FIG. 8. Axial light intensity of two helium I lines as dependent on the afterglow time in  $\mu\text{sec}$ .

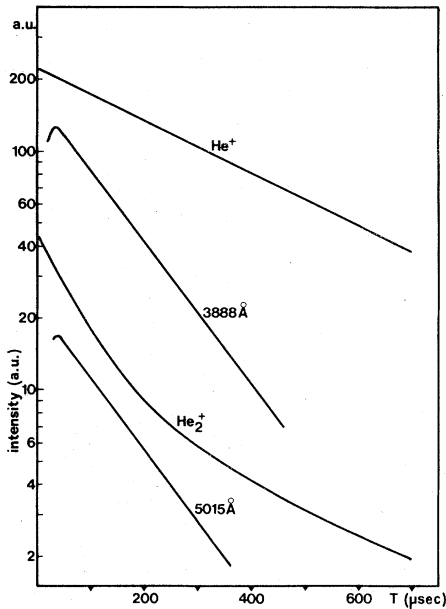


FIG. 9. Semilogarithmic decay curves of the ion densities of  $\text{He}^+$  and  $\text{He}_2^+$  and of the light intensity of the He I 3888-Å and the He I 5015-Å lines with afterglow time  $T$  in  $\mu\text{sec}$ .

same time constant as  $\text{He}^+$  but does not contribute appreciably to the population of atomic He states.

It is now interesting to compare the population of the upper states of the observed lines in the afterglow with the population measured in the active discharge, as described in Sec. IIIA. Figure 10

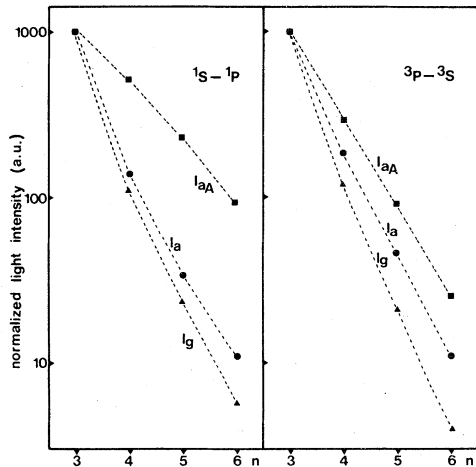


FIG. 10. Comparison of the light intensity, normalized at the principal quantum number value  $n = 3$ , for the  $n s^1 S - 2 p^1 P$  and the  $n p^3 P - 2 s^1 S$  series of He I as dependent on the quantum number  $n$ .  $I_a$  is the light intensity on the axis,  $I_g$  the light intensity at the glow edge, both for the active phase of the discharge.  $I_{aA}$  is the axial light intensity in the afterglow at time  $T = 100 \mu\text{sec}$ .

shows such a comparison for the  $1S-1P$  and  $3P-3S$  series, normalized to the  $n = 3$  level. The steepest curves show the population of the levels on the axis at low pressures and on the glow edge at all pressures in the active discharge. This population corresponds to the electron impact excitation by fast electrons. The middle curve shows the population on the axis in the active discharge at 4 Torr and 25 mA, the uppermost one the axial population in the afterglow after 100  $\mu\text{sec}$ . The relative increase in the population of the higher states on the axis with higher pressure in the active discharge toward the values obtained in the afterglow is a clear evidence of the population by recombination as this is the only important process (in the afterglow, the fast electrons have gone away completely). For the singlet lines, the approach of the afterglow values is somewhat slower, as is indicated in Fig. 10(a). This has been observed already in the active phase (Sec. IIIA), where the increase of the axial intensity of triplet lines emitted from higher states was much more pronounced as compared with the singlet lines. There is some uncertainty in the determination of these curves as the absolute response of the entire photon measuring equipment must be known. Before calculating the relative populations, the sensitivity has been corrected (the wavelength region extends from 2829 to 7065 Å, with sensitivity changes of a factor of 15).

D. Ionic helium lines

In addition to the study of the atomic He lines, the intensity distribution of ionic He II lines has been recorded in the radial coordinate at various pressure and discharge current values. Figure 11 shows two examples of the 4685 Å  $4f^2 F - 3d^2 D$  and the 3203 Å  $5f^2 F - 3d^2 D$  lines at a pressure of 1.7 Torr and discharge current values of 10, 13, 16, 22, and 25 mA. The distributions look exactly alike indicating that there is no difference in the excitation mechanism dependent on the principal quantum number of the state. The most pronounced feature of these curves is the negative or  $1/r$  curvature, which is an image of the concentration of the electron density of the fast electrons toward the axis out of simple geometric reasons. In contrast to the excitation energies of the atomic lines, which peak all at about 40 eV (Ref. 14), which means that one cathode-sheath electron of an energy of 100–400 eV can excite many atoms one after the other, the excitation energies of He to produce excited  $\text{He}^+$  states peak around 200 eV (Ref. 16) so that only unscattered electrons which have never undergone any collisions are able to excite these states. Originally the electrons are

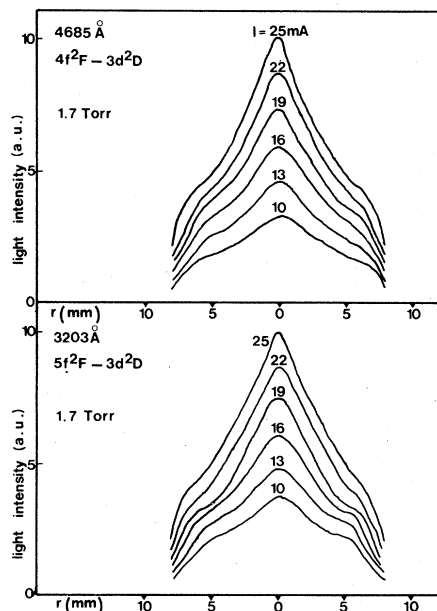


FIG. 11. Radial light intensity distribution for two He II lines at a discharge pressure of 1.7 Torr and at discharge current values of 10, 13, 16, 19, 22, and 25 mA in the active phase of the discharge.

directed toward the axis by the radial field in the cathode sheath. If they can keep this direction by not being scattered and then hit an atom, the possibility of ionizing and exciting at the same time is given. The excited ions have short lifetimes and radiate immediately, their emission pattern being a true picture of the density distribution of the exciting electron species. Ground-state He<sup>+</sup> ions on the other hand have time to diffuse so that the density distribution of excited ions differs very much from that of ground-state ions as depicted in Fig. 6. At higher pressures the He<sup>+</sup> density pattern remains the same but the intensity ratios on the axis and on the glow edge show nonlinearities with the discharge current and pressure which are indicative of the sensitivity of the radial concentration of this exotic electron group to the discharge parameters. For the development of hollow-cathode charge exchange lasers these nonlinearities have been already noted and their importance was underlined.<sup>17</sup> The contribution of the unscattered electrons to the total fast-electron density must be very small otherwise the curves of Sec. IIIA would not be understandable.

#### IV. DISCUSSION

From the radial distribution of the He I lines at low pressure (2 Torr) it is evident that the bulk of the discharge is excited by one group of fast electrons. A selective excitation of different levels

is not to be expected according to the electron-energy dependence of the excitation cross sections as measured by St. John *et al.*<sup>14</sup> The excitation prefers the lower states and the higher states are populated almost exponentially less with increasing principal quantum number.

Recombination as a means of populating the higher states is not yet a significant process as the electron temperature is too high at the low pressures around 2 Torr. The same remarks still hold true for higher pressures (4 Torr) and low discharge currents (around 10 mA). Now the plasma electron density is still too low for effective recombination of the atomic helium ions. Only when the discharge current is high enough, recombination into the higher levels becomes important. The discharge current dependence of the relative light intensity on the axis,  $I_a$  (where there are the slow plasma electrons which promote recombination) as compared to the one at the glow edge  $I_g$  (only fast electrons), shows a faster-than-linear increase. That is an indication for dielectronic recombination to be the main population mechanism there.

The pressure dependence of the intensity ratio  $I_a/I_g$  again shows the importance of thermalization of the plasma electrons with pressure. Only at sufficiently high pressure does the principal quantum-number order of the upper states reverse, indicating the increasing importance of recombination.

In the afterglow, thermalization has been completed after about 100 microseconds. The relative population for the states with higher principal quantum number now is highest, with the values at 25-mA discharge current (active discharge) and a pressure of 4 Torr lying in between the numbers for electron excitation alone (active discharge) and those for recombination (afterglow phase). That means that even at 4 Torr the electrons are only partially thermalized in the active phase of the discharge.

The end state of all the observed triplet lines is the metastable  $2s^3S$  state; after electronic conversion of the  $2s^1S$  state it is also the end state of the singlet series. Therefore the dielectronic recombination of He<sup>+</sup> is an effective process of metastable production on the axis of a hollow cathode, at least at high pressure. This observation is important for the development of the hollow cathode into an effective excitation transfer laser.

A second process that might be important for the hollow-cathode-laser development is the  $1/r$  increase of the group of fast electrons which have never undergone a collision on their way from the cathode wall to the axis of the discharge. This provides an excellent means of producing excited

ions whose excitation energy lies too high for ordinary fast electrons in the discharge. The spatial electron density distributions inferred from the intensity distribution of excited helium ions shows the high excitation conditions on the axis where a hollow-cathode laser is expected to work most effectively. Similar distributions have been observed by studying the spatial density distribution

of highly charged krypton ions mass spectrometrically in a krypton hollow-cathode discharge.<sup>9</sup>

#### ACKNOWLEDGMENTS

The study was partially supported by the Fonds zur Förderung der wissenschaftlichen Forschung in Österreich under Project No. S-18/06.

- 
- <sup>1</sup>H. J. Oskam, in *Case Studies in Atomic Collisions Physics*, edited by E. W. McDaniel and M. R. C. McDowell (North-Holland, Amsterdam/London, 1969), Vol. I, p. 465.
- <sup>2</sup>H. S. W. Massey and H. B. Gilbody, *Recombination, Electronic and Ionic Impact Phenomena*, 2nd ed., Vol. IV, *Recombination and Fast Collisions of Heavy Particles* (Oxford University Press, New York, 1974), p. 2115.
- <sup>3</sup>R. Deloche, P. Monchicourt, M. Cheret, and F. Lambert, *Phys. Rev. A* **13**, 1140 (1976).
- <sup>4</sup>M. Pahl (private communication).
- <sup>5</sup>W. Lindinger, *Phys. Rev. A* **7**, 328 (1973).
- <sup>6</sup>F. Howorka, *J. Chem. Phys.* **64**, 5313 (1976); **64**, 2919 (1977); **68**, 804 (1978).
- <sup>7</sup>F. Howorka, W. Lindinger, and R. N. Varney, *J. Chem. Phys.* **61**, 1180 (1974).
- <sup>8</sup>I. Kuen, F. Howorka, and R. N. Varney, *Int. J. Mass Spectrom. Ion Phys.* **28**, 101 (1978).
- <sup>9</sup>F. Howorka and I. Kuen, *J. Chem. Phys.* **70**, 758 (1979).
- <sup>10</sup>I. Kuen and F. Howorka, *J. Chem. Phys.* **70**, 595 (1979).
- <sup>11</sup>F. Howorka, A. Scherleitner, V. Gieseke, and I. Kuen, *Int. J. Mass Spectrom. Ion Phys.* **32**, 321 (1980).
- <sup>12</sup>H. Störi, T. D. Märk, M. Langenwaller, and M. Pahl, *J. Phys. E* **9**, 917 (1976).
- <sup>13</sup>H. Störi, T. D. Märk, R. N. Varney, and M. Pahl, *Beitr. Plasmaphys.* **18**, 79 (1978).
- <sup>14</sup>R. M. St. John, S. F. Miller, and C. C. Lin, *Phys. Rev.* **134**, A888 (1964).
- <sup>15</sup>R. A. Gerber, G. F. Sauter, and H. J. Oskam, *Physica (Utrecht)* **32**, 2173 (1966).
- <sup>16</sup>H. M. Moussa and F. J. de Heer, *Physica (Utrecht)* **36**, 646 (1967).
- <sup>17</sup>K. Rózsa (unpublished).